A Three-Dimensional Finger-Tapping Framework for Recognition of Patients With Mild Parkinson's Disease

Junjie Li, *Student Member, IEEE*, Huaiyu Zhu, *Member, IEEE*, Haotian Wang, Bo Wang, Zhidong Cen, Dehao Yang, Peng Liu, Wei Luo, and Yun Pan, *Member, IEEE*

***Abstract*— The finger tapping test is a widely-used and important examination in the Movement Disorder Society Clinical Diagnosis for Parkinson's Disease. However, finger tapping motion could be affected by age, medication, and other conditions. As a result, Parkinson's disease patients with mild sign and healthy people could be rated as similar scores on the Movement Disorder Society-sponsored revision of the Unified Parkinson's Disease Rating Scale, making it difficult for community doctors to perform diagnosis. We therefore propose a three-dimensional finger tapping framework to recognize mild PD patients. Specifically, we first derive the three-dimensional finger-tapping motion using a self-designed three-dimensional finger-tapping measurement system. We then propose a three-dimensional finger-tapping segmentation algorithm to segment three-dimensional finger tapping motion. We next extract three-dimensional pattern features of motor coordination, imbalance impairment, and entropy. We finally adopted the support vector machine as the classifier to recognize PD patients. We evaluated the proposed framework on 49 PD patients and 29 healthy controls and reached an accuracy of 94.9% for the right hand and 89.4% for the left hand. Moreover, the proposed framework reached an accuracy of 95.0% for the right hand and 97.8% for the left hand on 17 mild PD patients and 28 healthy controls who were both rated as 0 or 1 on the Movement Disorder Society-sponsored revision of the Unified Parkinson's Disease Rating Scale. The results demonstrated that the proposed framework was less sensitive to traditional features and performed well in recognizing mild PD patients by involving three-dimensional patter features.**

Manuscript received 28 November 2022; revised 26 April 2023; accepted 14 July 2023. Date of publication 26 July 2023; date of current version 22 August 2023. This work was supported in part by the Zhejiang Provincial Key Research and Development Program under Grant 2021C03027, in part by the Zhejiang Provincial Natural Science Foundation of China under Grant LQ21F010016, and in part by the Key Laboratory of Collaborative Sensing and Autonomous Unmanned Systems of Zhejiang Province. *(Corresponding author: Yun Pan.)*

This work involved human subjects or animals in its research. Approval of all ethical and experimental procedures and protocols was granted by the Ethics Committee of the Second Affiliated Hospital of Zhejiang University School of Medicine under Application No. 2019-287.

Junjie Li, Huaiyu Zhu, and Yun Pan are with the College of Information Science and Electronic Engineering, Zhejiang University, Hangzhou 310027, China (e-mail: panyun@zju.edu.cn).

Haotian Wang, Bo Wang, Zhidong Cen, Dehao Yang, Peng Liu, and Wei Luo are with the Department of Neurology, Second Affiliated Hospital, School of Medicine, Zhejiang University, Hangzhou 310027, China.

Digital Object Identifier 10.1109/TNSRE.2023.3296883

***Index Terms*— Parkinson's disease, finger tapping, three-dimensional, machine learning.**

I. Introduction

THE finger tapping (FT) test is an easy task with little time cost and widely-used for the evaluation of motor function in clinical practice, especially in screening. It is an important part of the Movement Disorder Society Clinical Diagnostic Criteria for Parkinson's Disease [1] to assess the bradykinesia of upper limbs. Moreover, Agostino [2] reported that PD patients performed FT test significantly difficult than the other upper-limb tests for bradykinesia assessment. The FT test is thus important for the diagnosis of Parkinson's disease (PD). In clinical practice, neurologists investigate hypokinesia, fatigue, and especially slowness in evaluating FT on a five-point scale from 0 to 4 according to the Movement Disorder Society-sponsored revision of the Unified Parkinson's Disease Rating Scale (MDS-UPDRS) [3], where a zero value indicates normal and a value of 4 indicates severe symptom [3].

Other conditions, e.g. age and medication status, might affect the FT motion significantly [4]. For example, healthy people might suffer from motor impairment due to aging [5] and Levodopa could be used to treat PD patients effectively. As a result, healthy people might be rated as 1 or above owing to aging in the FT test [3], whereas PD patients might be rated as 0 in the ON state. The overlap between healthy people with aging and PD patients leads to low accuracy ($75-85\%$) in the diagnosis of Parkinson's disease in the community [6], [7]. In particular, the FT score of mild PD patients might be similar to that of healthy people. Thus, identifying mild PD patients by FT task is challenging. Moreover, identifying mild PD patients is important because the early diagnosis and treatment of PD can reduce the risk of dyskinesia and greatly increase quality of life [8].

Ways of identifying mild PD patients from healthy people with aging-related motor decline can be summarized as conducting more test, adopting normalization, and using new features. More tests could be conducted to assess other motor symptoms of PD, e.g. bradykinesia of low limb, rest tremor, and rigidity [1]. Those tests are widely used in clinical practice

This work is licensed under a Creative Commons Attribution-NonCommercial-NoDerivatives 4.0 License.
For more information, see https://creativecommons.org/licenses/by-nc-nd/4.0/

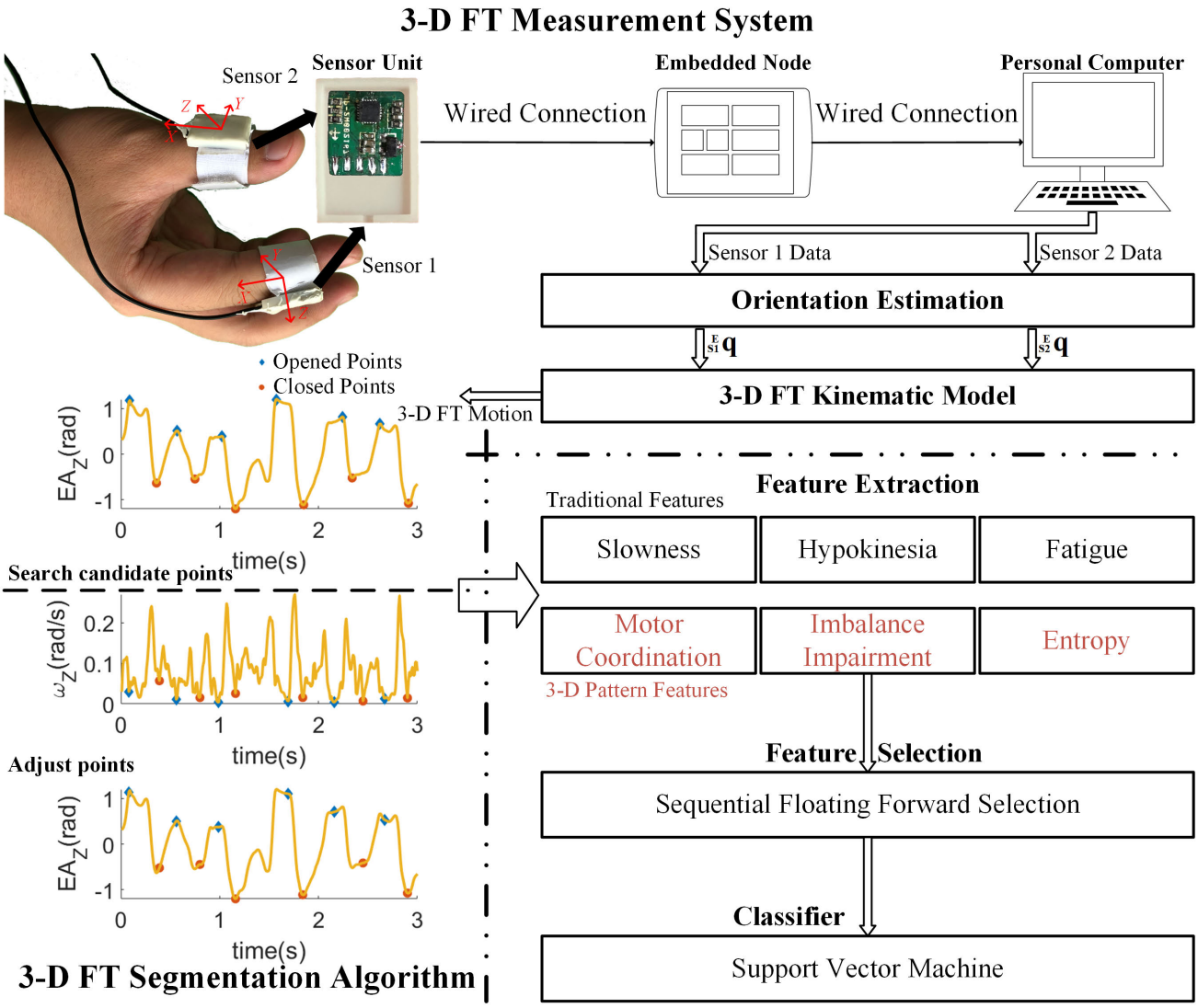

Fig. 1. Overview of the proposed three-dimensional finger-tapping assessment framework.

but time consuming. The effect of age can be removed through normalization method [9]. However, this method requires a large data set including healthy people of different ages and could not deal with nonlinear effect. New features not sensitive to traditional features can potentially be used to identify mild PD patients, which was also mentioned in the Movement Disorder Society Clinical Diagnostic Criteria [1]. We speculated that those new features should be dimensionless and described FT motion in other ways to reduce the effects of age and symptom severity.

Most recent studies [4], [10], [11], [12], [13], [14], [15], [16] have simplified FT motion as a scissors-like motion. This simplification ignores the multi-joints motion of FT, which makes it impossible to analyze the multi-joints pattern of the FT. To analyze the multi-joints pattern, we proposed a three-dimensional (3-D) finger tapping measurement system and extracted 3-D pattern features in our previous work [17]. As a result, we found that 3-D pattern features were more significant than one-dimensional (1-D) features between mild PD patients and healthy people [17].

In this study, we propose a 3-D finger-tapping assessment framework for recognition of PD patients, especially mild PD patients. The overview of the proposed framework was shown in Fig. 1. Firstly, we collected 3-D FT motion data using our 3-D FT measurement system [17]. Specifically, we collected motion data of the thumb and forefinger using sensor units, estimated the orientation of sensor units ($^{E}_{S1}\mathbf{q}$ and $^{E}_{S2}\mathbf{q}$) using Mahony's complementary filter [18], and derived 3-D FT motion using our 3-D kinematic model. Second, we searched for candidate segmentation points by peak searching method and adjusted these points by combing the magnitude of angular velocity with the rotation angle. We thus obtained the closed and opened points of each tapping and segmented 3-D FT motion. In feature extraction, we combined slowness, hypokinesia, and fatigue features with the proposed 3-D pattern features, namely motor coordination, imbalance impairment, and entropy features. Third, we used sequential floating forward selection method [19] to select features and avoid the curse of dimensionality. Finally, we used support vector machine [20] as the classifier to recognize PD patients. We evaluated the

proposed framework on 49 PD patients and 29 healthy controls (HC). The proposed framework reached an accuracy of 94.9% for the right hand and accuracy of 89.4% for the left hand on the total data set. On the data subset in which both PD patients and HC were rated as 0 or 1 according to the MDS-UPDRS, the accuracy for right hand was 95.0% and the accuracy for left hand was 97.8%. The results demonstrated that the proposed framework worked better in recognizing mild PD with the inclusion of 3-D pattern features.

A. Related Work

Several research groups have used various sensors to recognize PD patients. Lones et al. [4], Gao et al. [11], and Dai et al. [16] adopted electromagnetic devices to collect FT motion. Krupicka et al. [10] proposed the BradyAn system to analyze FT, hand movements, and pronation-supination movements using optical sensors. Butt et al. [12] and Buongiorno et al. [13] used Leap Motion sensors to collect the hand motion. Moshkova et al. [14] adopted Kinect v2 to collect gait, FT, and foot tapping motions. Park et al. [15] adopted wearable inertial sensors to collect FT, hand movement, and rapid alternating movements.

Most related works have simplified FT motion as a scissors-like motion, i.e. the flexion/extension angle of the forefinger [15] or the distance between the thumb and forefinger [4], [10], [11], [12], [13], [14], [16]. Through this simplification, the studies simply analyzed 1-D FT motion and ignored multi-joints FT motion. Especially, although Djuric-Jovicic et al. [21] considered FT motion as a 3-D movement, they still described FT motion as the rotation around the dominant axis to simplify FT to a single scalar value. Therefore, these works could not analyze the multi-joints pattern of the FT.

As for FT features, most researchers [10], [12], [13], [14], [15], [16] tried to find better features relating to slowness, hypokinesia, and fatigue. As an example, Yokoe [22] proposed the opening velocity proposed to describe slowness. Besides, Lone [4] and Gao [11] adopted Cartesian genetic programming to obtain FT features implicitly and found that PD patients slowed their fingers prior to the inelastic point. Two task types, namely horizontal [12], [21] and vertical [4], [10], [11], [12], [13], [14], [16], have been adopted by related works but the effect of the task type remains unclear.

In summary, to the best of our knowledge, no previous research has focused on distinguishing mild PD patients from those healthy people with aging-related motor decline using only a single FT motion.

B. Contributions and Article Structure

The main contributions of this study are as follows:

- Proposing a 3-D finger-tapping assessment framework for the analysis of the multi-joints motion of finger tapping;
- Testing the effect of task type on 3-D pattern features and finding the horizontal tasks might be a better choice for the recognition of mild PD patients;
- Involving 3-D pattern features and achieving better performance in distinguishing mild PD patients from healthy people with aging-related motor decline.

The remainder of this paper is organized as follows. In section II, we describe the proposed 3-D finger-tapping assessment framework in detail. In section III, we introduce the validation experiment and present the results for the proposed framework. In section IV, we discuss the comparisons with related work, the analysis of 3-D pattern features, the effect of task type, the effect of dominant hand, and study limitation.

II. Three-Dimensional Finger-Tapping Assessment Framework

A. Three-Dimensional Finger-Tapping Measurement System

We previously proposed a 3-D FT measurement system in [17], which could collect 3-D FT motion with lightweight sensor units. In this paper, we adopted this measurement system to derive the 3-D FT motion and relative angular velocity with respect to the local coordination system of the thumb. Notably, we transformed the 3-D FT motion into the Euler angles in the order of Z-Y-X for interpretability. Thus, the Z and X components were mostly contributed by the forefinger and thumb respectively and we could analyze the imbalance impairment between the thumb and forefinger.

Especially, we adopted the local coordination system of the thumb in the zero position, i.e. we assumed the local coordination system of the thumb was parallel to the sensor 1, in our previous work [17], whereas Djuric-Jovicicet al. [21] adopted the local coordination system of the forefinger in the zero position. Therefore, the Z axis represents the motion of the thumb in Milica's model, but the motion of the forefinger in our model. We tested the performances of the proposed model and Milica's model [21] with the participant only moving the thumb or forefinger. To avoid the effect of the inconsistency of the coordinate systems of Milica's model and our model, we defined the energy ratio (**ER**) and the energy concentration (EC) to evaluate Milica's model and our model. **ER** and EC were derived as

$$\mathbf{ER} = \frac{(\sum_t EA_X(t)^2, \sum_t EA_Y(t)^2, \sum_t EA_Z(t)^2)}{\sum_t EA_X(t)^2 + EA_Y(t)^2 + EA_Z(t)^2}, \quad (1)$$

$$EC = \max_{j\in\{X,Y,Z\}} ER_j, \quad (2)$$

where EA_X, EA_Y, and EA_Z are the rotation angles around the X, Y, and Z axes respectively. As we assumed that a single component of the Euler angle represented the motion of one finger, the energy concentrations of the thumb and forefinger motions should both be sufficiently high. In addition, the cosine similarity between energy ratio of the thumb and forefinger motions should be small enough to separate the thumb and forefinger motions as much as possible for multi-joints pattern analysis.

The Table I showed that the energy concentration of the proposed model was above 0.4 for both the thumb and forefinger motions, whereas the energy concentration of Milica's model was below 0.4 for the forefinger. In terms of similarity, the proposed model also performed better than Milica's model. Overall, the results showed that the proposed 3-D kinematical model performed better for multi-joints pattern analysis.

TABLE I
COMPARISON BETWEEN MILICA'S MODEL AND OUR MODEL

Model	Finger	Energy Concentration	Similarity
Milica [21]	Thumb	0.64	0.30
	Forefinger	0.38	
Ours	Thumb	0.43	0.28
	Forefinger	0.59	

The similarity is the cosine similarity between the thumb motion and forefinger motions.

B. Three-Dimensional Finger-Tapping Segmentation Algorithm

The extraction of features relating to fatigue, opening velocity, and closing velocity requires the segmentation of FT motion. However, 3-D FT motion segmentation might be difficult because the thumb does not arrive at closed points and opened points at the same moment as the forefinger. To solve this problem, we propose a 3-D FT segmentation algorithm. The detail of the proposed algorithm was presented in the appendix.

As shown in Fig. 1 and Algorithm 1, the 3-D FT segmentation algorithm comprises two steps: searching for candidate points and then adjusting the points. We firstly applied peak searching method on the rotation angle around the Z axis to search for candidate points preliminarily because the forefinger generally contributes more than the thumb to FT motion [21]. Specifically, we determined the minimum peak prominence by (3) and determined the minimum peak distance by (4). We had

$$MPP = \alpha * iqr_Z, \tag{3}$$

$$MPD = \beta / f_p, \tag{4}$$

where MPP and MPD are respectively the minimum peak prominence and the minimum peak distance in peak searching method; iqr_Z is the inter quartile range of the rotation angle around the Z axis; f_p is the peak frequency of the rotation angle around the Z axis; α, and β are the search parameters.

Notably, the coordination system differed between the left hand and the right hand owing to mirror symmetry between the left and right hands. As a result, the peaks of the rotation angle around the Z axis of the left and right hands are correspond to closed and opened points respectively.

We then used the magnitude of the relative angular velocity to adjust the times of the opened and the closed points as shown in Algorithm 1. First, we obtained a points set ($\mathbb{M}$) by searching for the local minimums of the magnitude of the relative angular velocity, because the magnitude of the relative angle velocity at the opened and closed points should be local minimums around zero. Moreover, we derived the opened and closed points by maximizing the objective function (F) which combined the rotation angle around the Z axis and the magnitude of the relative angular velocity with the peak adjusting factor ($factor$).

We adopted the 3-D FT motion from the first closed point to the last closed point in the following analysis. In addition, we derived the maximum opening velocity, maximum closing velocity, and frequency of each tapping using the opened and closed points. The segmentation parameters, i.e. α, β, and $factor$, were determined in the validation experiment.

Algorithm 1 Three-dimensional Finger-Tapping segmentation Algorithm

Symbol Setting:
EA_Z: rotation angle around the Z axis.
$|\omega|$: magnitude of the relative angular velocity.
f_p: peak frequency of EA_Z.
iqr_Z: inter quartile range of EA_Z.
O_i, C_i: time of the i^{th} opened and closed points respectively
α, β: searching parameters.
$factor$: peak adjusting parameter.
MPD: minimum peak distance in peak searching.
MPP: minimum peak prominence.
F: objective function.
$\mathbb{M}$: local minimums set of $|\omega|$.

Process:
Let $MPP \leftarrow \alpha * iqr_Z$, $MPD \leftarrow \beta / f_p$.
if right hand **then**
  Let $angle \leftarrow -EA_Z$.
else
  Let $angle \leftarrow EA_Z$.
end if
Search local maximums of $angle$ with MPD and MPP.
Let $\mathbb{C} \leftarrow$ the time of those local maximums.
Let $N \leftarrow |\mathbb{C}|$.
for i from 1 to $N-1$ **do**
  Let $O_i \leftarrow$ minimum time of $angle$ from C_i to C_{i+1}.
end for
for i from 2 to $2N-2$ **do**
  if (i is odd && right hand)||(i is even &&left hand) **then**
    Let $F \leftarrow -Norm(|\omega|) - factor * Norm(EA_Z)$.
  else
    Let $F \leftarrow -Norm(|\omega|) + factor * Norm(EA_Z)$.
  end if
  if i is odd **then**
    Let $\mathbb{M} \leftarrow$ local min of $|\omega|$ from $O_{0.5*i-0.5}$ to $O_{0.5*i+0.5}$.
    Let $C_{0.5*i+0.5)} \leftarrow argmax(F(\mathbb{M}))$.
  else
    Let $\mathbb{M} \leftarrow$ local min of $|\omega|$ from $C_{0.5*i}$ to $C_{0.5*i+1}$.
    Let $O_{0.5*i} \leftarrow argmax(F(\mathbb{M}))$.
  end if
end for

C. Feature Extraction

Referring to the MDS-UPDRS [3], neurologists recognize the FT motion of PD patients by slowness, hypokinesia, and fatigue in clinical practice. In this study, we combined these traditional features with the proposed 3-D pattern feature. To analyze the feature contributions, we divided the extracted features into 6 feature groups, namely slowness, hypokinesia, fatigue, motor coordination, imbalance impairment, and entropy, according to the physical meanings of these features. In total, we extracted 32 features: 4 slowness features,

3 hypokinesia features, 11 fatigue features, 8 motor coordination features, 3 imbalance impairment features, and 3 entropy features.

We assessed slowness by tapping frequency and angle velocity. Specifically, we adopted the mean tapping frequency, root mean square of the angular velocity, root mean square of the opening angular velocity, and root mean square of the closing angular velocity. Hypokinesia is smaller amplitude of movement [23], and we assessed hypokinesia using the mean range of the rotation angle around the X, Y, and Z axes for each tapping. Fatigue is the decrements of speed and amplitude in FT test. We assessed fatigue using the standard deviation of the tapping frequency, coefficients of variation of the Euler angles, maximum opening velocity, and maximum closing velocity. We also used the decrement of Euler angles, maximum opening velocity, and maximum closing velocity to assess fatigue.

Motor coordination relates to the smoothness of multi-joints motion. Specifically, we adopted the number of local minimums with respect to the magnitude of the relative angular velocity, the normalized first principal component variances of the relative angular velocity, and the correlation between all components of the relative angular velocity. We derived the normalized first principal component variances of the relative angular velocity by

$$\frac{\lambda_1}{\lambda_1+\lambda_2+\lambda_3}, \tag{5}$$

where λ_i is the i^{th} principal component variances of the relative angular velocity. In addition, we adopted spectral coherence analysis to estimate the correlation between all components of the relative angular velocity. Taking the correlation between X and Z component as an example, we derived C_{XZ} by

$$C_{XZ}=\frac{P_{XZ}}{\sqrt{P_{XX}*P_{ZZ}}}, \tag{6}$$

where P_{XX} and P_{ZZ} are respectively the autocorrelation spectrum of the X and Z components of the relative angular velocity; P_{XZ} is the cross-power spectrum for the X and Z components of the relative angular velocity. We then adopted the maximum and the peak number of C_{XZ} to estimate the correlation between the X and Z component of the relative angular velocity.

This study considered imbalance impairment in early PD: the imbalance impairment between the thumb and forefinger and the imbalance impairment between the opening and closing motions. We assessed the imbalance impairment between the thumb and forefinger using the relative thumb angular velocity by (7) and relative thumb range of motion by (8):

$$\frac{rms(\omega^X)}{rms(|\boldsymbol{\omega}|)}, \tag{7}$$

$$\frac{DRX}{\sqrt{DRX^2+DRY^2+DRZ^2}}, \tag{8}$$

where ω^X is the X component of the relative angular velocity; $\boldsymbol{\omega}$ is the relative angular velocity; DRX, DRY, and DRZ are respectively the ranges of the rotation angles around the X, Y, and Z axes. Meanwhile, we assessed the imbalance impairment between the opening and closing motions by

$$\frac{rms(|\boldsymbol{\omega_{opening}}|)}{rms(|\boldsymbol{\omega_{closing}}|)}, \tag{9}$$

where $\boldsymbol{\omega_{opening}}$ and $\boldsymbol{\omega_{closeing}}$ are respectively the relative angular velocities during opening and closing procedures.

Entropy features relate to the complexity of the relative angular velocity, as inspired by the roller bearing fault diagnosis [24]. We adopted variational mode decomposition [25] to decompose the components of the relative angular velocity and obtained the energy entropy, and we derived the variational mode decomposition energy entropy of all components of the relative angular velocity. Taking the Z component as an example, we derived the variational mode decomposition energy entropy as

$$-\sum_{i=1}^{5}\frac{V_i^{\omega^Z}}{\sum_{i=1}^{5}V_i^{\omega^Z}}\log\frac{V_i^{\omega^Z}}{\sum_{i=1}^{5}V_i^{\omega^Z}}, \tag{10}$$

where $V_i^{\omega^Z}$ is the energy of the i^{th} intrinsic mode function of the Z component of the relative angular velocity.

To compare the performance between 1-D and 3-D features, we extracted 1-D features from the motion of forefinger (i.e. the Z component of the relative angular velocity and the rotation angle around the Z axis) referring to [21]. In total, we extracted 15 1-D features. Specifically, we extracted the mean tapping frequency and root mean square of the Z component of the relative angular velocity, the opening angular velocity, and the closing angular velocity to assess slowness; mean range of the rotation angle around the Z axis to assess hypokinesia; standard deviation of the tapping frequency, coefficients of variation and decrement of range of the rotation angle around the Z axis, the maximum of the Z component of the opening angular velocity, and the maximum of the Z component of the closing angular velocity to assess fatigue; the zero crossing number of the Z component of the relative angular velocity to assess motor coordination; ratio between the forefinger opening and closing velocities to assess imbalance impairment; and variational mode decomposition energy entropy of the Z component of the relative angular velocity to assess entropy. There are no corresponding 1-D forms of the normalized first principal component variances of the relative angular velocity and the correlation between components of the relative angular velocity. Thus, we did not include these features. Notably, we also used the 3-D segmentation results in 1-D feature extraction to allow the comparison of the 1-D features and 3-D feature.

D. Feature Selection and Classification

To avoid the dimensional disaster, we normalized features using z-scores and adopted the sequential floating forward selection method for feature selection. We adopted this method to get the final feature set because its set is not fixed, which could eliminate the nesting problem [19].

For each task, we used the support vector machine [20] to distinguish PD patients from HC, considering the limitation of

TABLE II
DEMOGRAPHIC AND CLINICAL DATA OF THE TOTAL DATA SET

Variables	PD	HC	p-value
Sample N	49	29	
Gender: No. male/female	31/18	13/16	0.1566[a]
Age: years (mean±SD)	55.9±8.3	54.4±8.2	0.4400[b]
Onset side: No. left/right/unclear	24/22/3	/	/
Left FT Score: No. 0/1/2/3	7/15/19/8	17/12/0/0	<0.0001[c]
Right FT Score: No. 0/1/2/3	7/18/18/6	18/10/1/0	<0.0001[c]

The onset side is the side on which initial symptoms appeared.
[a] Fisher exact test.
[b] t-test.
[c] Kruskal-Wallis test; this test was adopted because assumptions of normality and homogeneity of variance were not satisfied.

TABLE III
DEMOGRAPHIC AND CLINICAL DATA OF THE *noSeverePD* SUBSET

Variables	PD	HC	p-value
Sample N	17	28	
Gender: No. male/female	6/5	13/15	0.7311[a]
Age: years (mean±SD)	57.2±7.7	54.5±8.4	0.3134[c]
Onset side: No. left/right/unclear	5/11/1	/	/
Left FT Score: No. 0/1	7/10	17/11	0.2079[c]
Right FT Score: No. 0/1	7/10	18/10	0.1347[c]

The onset side is the side on which initial symptoms appeared.
[a] Fisher exact test.
[c] Kruskal-Wallis test; this test was adopted because assumptions of normality and homogeneity of variance were not satisfied.

the sample size. The radial basis function kernel was adopted because it is generally a reasonable choice [26]. We adopted the grid search method to find the optimal hyper-parameter of the support vector machine as recommended in [20]. To evaluate the performance of our framework, we conducted a five-fold cross-validation in which each subject was tested once.

III. VALIDATION EXPERIMENT

A. Data Collection Protocol

The experiment was approved by the Ethics Committee of the Second Affiliated Hospital of Zhejiang University School of Medicine (2019-287). Forty-nine PD patients and 29 HC participated in the experiment. The inclusion criteria were: (1) a firm diagnosis of PD according to the Movement Disorder Society Clinical Diagnostic Criteria for PD patients [1], (2) no movement disorder disease for HC as judged by neurologists, and (3) an age between 40 and 70 for all participants. The exclusion criteria were: (1) people who could not finish FT tasks, (2) people who were left-handed, and (3) people suffering from demented, depressed, or any other neurological disease. The demographic and clinical data of all participants are summarized in the Table II.

In the experiment, we designed four FT tasks: namely the left-hand horizontal task, left-hand vertical task, right-hand horizontal task, and right-hand vertical task. Each task was recorded for 10 seconds. when performing horizontal tasks, participants were instructed to put their hands on the desktop and move their fingers parallel to the desktop referring to [21], [22], and [27]. When performing vertical tasks, participants were instructed to raise their arms with their palms forward [3]. During data collection, participants performed the left-hand horizontal task, left-hand vertical task, right-hand horizontal task, and right-hand vertical task in order. And participants were asked to rest between tasks to avoid the effect of the task order. An independent neurologist evaluated the FT for the vertical tasks on MDS-UPDRS [3] and dervied MDS-UPDRS FT scores. Especially, we did not collect the scores of the rest tests of the MDS-UPDRS to reduce time cost, because there is not a single cutoff of MDS-UPDRS could be used to define PD according to the Movement Disorder Society Clinical Diagnostic Criteria for PD [1].

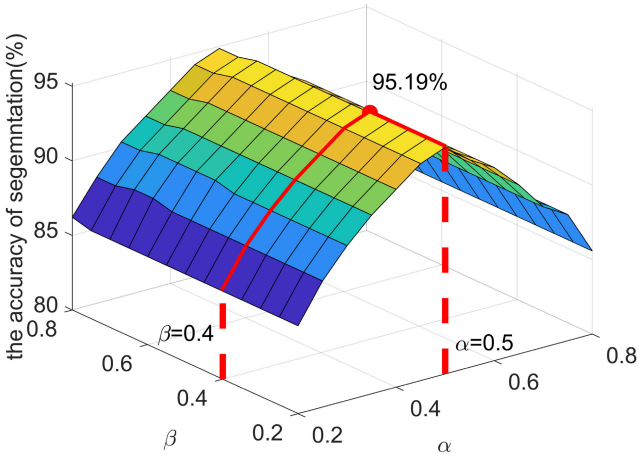

Fig. 2. Results of the grid search in segmentation.

Notably, we established one data subset, namely *noSeverePD*, to investigate the performance of the framework in distinguishing mild PD patients from HC. The *noSeverePD* included all HC and PD patients rated as 0 or 1 for both the left and right hands. The demographic and clinical data of the *noSeverePD* subset are listed in the Table III. This table shows that no singificant difference in the FT scores between mild PD patients and HC in the *noSeverePD* subset. We thus obtained the *noSeverePD* subset in which PD patients and HC were rated as similar MDS-UPDRS FT scores.

B. Segmentation Results

We first determined $factor$ by investigating the reasonable opened and closed points with $\alpha = 0.5, \beta = 0.5$, because the parameter $factor$ did not affect the results of tapping counts. After investigating several samples, we set $factor = 0.6$. We then conducted a grid search to determine α and β. A marginal effect might arise in searching for local maximums, because we only searched whole tapping from the first closed point to the last closed point. We thus defined the output as being correct when the difference between the output tapping count and the tapping count label was less than 2. We showed the results of the grid search in Fig. 2. We finally set $\alpha = 0.5, \beta = 0.4$ and achieved a segmentation accuracy of 95.19%. The results demonstrated the 3-D FT motion was reliable in view of the tapping counts.

TABLE IV
SIGNIFICANT FEATURES BETWEEN PD PATIENTS AND HC ON THE TOTAL DATA SET

Group	Feature	Results of Significance Testing			
		Left-hand vertical	Left-hand horizontal	Right-hand vertical	Right-hand horizontal
Slowness	mean tapping frequency	$*$	$*$	$*$	$*$
	root mean square of angular velocity	$*$	$*$	$*$	$*$
	root mean square of opening angular velocity	$*$	$*$	$+$	$*$
	root mean square of closing angular velocity	$*$	$*$	$*$	$*$
Hypokinesia	mean rotation range of angle around X axis	$+$	$-$	$-$	$+$
	mean range of rotation angle around Y axis	$*$	$*$	$+$	$+$
	mean range of rotation angle around Z axis	$-$	$+$	$-$	$*$
Fatigue	standard deviation of tapping frequency	$+$	$+$	$-$	$-$
	decrement of range of rotation angle around Y axis	$-$	$+$	$-$	$-$
	coefficient of variation of maximum opening velocity	$+$	$-$	$-$	$-$
	coefficient of variation of maximum closing velocity	$-$	$-$	$-$	$+$
	decrement of maximum opening velocity	$-$	$*$	$-$	$-$
	decrement of maximum closing velocity	$-$	$-$	$-$	$+$
Motor coordination	number of local minimums of $\|\omega\|$ less than lower quartile	$*$	$*$	$*$	$*$
	normalized first principal component variances of $\boldsymbol{\omega}$	$*$	$*$	$*$	$*$
	maximum of the the spectral coherence between ω^X and ω^Z	$-$	$*$	$-$	$-$
	peak number of the the spectral coherence between ω^X and ω^Z	$-$	$+$	$-$	$-$
Imbalance impairment	relative thumb angular velocity	$+$	$*$	$+$	$*$
	ratio between opening and closing velocities	$*$	$+$	$+$	$+$
Entropy	variational mode decomposition energy entropy of ω^X	$*$	$*$	$-$	$*$
	variational mode decomposition energy entropy of ω^Y	$-$	$*$	$-$	$*$
	variational mode decomposition energy entropy of ω^Z	$*$	$*$	$*$	$*$

We conducted the one-factor analysis of variance when the normality and homogeneity of variance assumptions were satisfied. Otherwise, we conducted the Kruskal-Wallis test.
ω refers to the relative angular velocity.
ω^X, ω^Y, and ω^Z refer to the X, Y, and Z components of the relative angular velocity.
"$-$" means "$p > 0.05$"; "$+$" means "$p < 0.05$"; "$*$" means "$p < 0.01$".

TABLE V
COMPARISON BETWEEN HORIZONTAL TASKS AND VERTICAL TASKS ON THE TOTAL DATA SET

Task	Sensitivity	Specificity	Accuracy	F1-Score
LV	$87.6 \pm 8.9\%$	$\mathbf{89.3 \pm 9.8\%}$	$88.5 \pm 6.2\%$	$90.2 \pm 5.2\%$
LH	$\mathbf{91.8 \pm 8.4\%}$	$86.7 \pm 13.9\%$	$\mathbf{89.4 \pm 7.0\%}$	$\mathbf{91.8 \pm 5.8\%}$
RV	$\mathbf{96.0 \pm 5.5\%}$	$76.0 \pm 18.8\%$	$88.5 \pm 5.0\%$	$91.5 \pm 3.3\%$
RH	$93.8 \pm 5.7\%$	$\mathbf{96.7 \pm 7.5\%}$	$\mathbf{94.9 \pm 5.3\%}$	$\mathbf{95.8 \pm 4.2\%}$

Numerical values are reported as mean value $\pm$ standard deviation of the five-fold results.
Bold font shows the higher value between horizontal and vertical tasks.
LV, LH, RV, and RH denote the left-hand vertical, left-hand horizontal, right-hand vertical, and right-hand horizontal tasks respectively.

C. Effect of the Task Type

We listed the results of significance testing between PD patients and HC on the total data set in the Table IV. This table showed that most features, except the mean range of the rotation angle around the X axis, coefficient of variation of the maximum of the opening velocity for each tapping, and ratio of the opening and closing velocities showed the same or greater difference between PD patients and HC in horizontal tasks compared with vertical tasks.

We also investigated the effect of the task type on distinguishing PD patients from HC as presented in the Table V. The performance of classification was better for horizontal tasks than vertical tasks for both left and right hands. We therefore only investigated horizontal tasks in the following analysis.

TABLE VI
RESULTS OF FEATURE SELECTION ON THE TOTAL DATA SET

Hand	Selected Features	r
Left	root mean square of angular velocity	-0.70
	variational mode decomposition energy entropy of ω^X	0.35
	standard deviation of tapping frequency	-0.29
	root mean square of closing angular velocity	-0.68
	peak number the spectral coherence between ω^X and ω^Y	0.44
	coefficient of variation of maximum closing velocity	0.33
	number of local minimums of $\|\omega\|$ less than lower quartile	0.59
Right	normalized first principal component variances of $\boldsymbol{\omega}$	-0.45
	variational mode decomposition energy entropy of ω^X	0.52
	relative thumb angular velocity	0.56
	coefficient of variation of range of EA_X	0.06
	decrement of range of EA_X	-0.17
	coefficient of variation of range of EA_Y	0.03
	mean range of EA_Y	-0.34

The selected features are listed in the order of the sequential floating forward selection method.
r is the Pearson correlation coefficient for the selected feature and MDS-UPDRS finger tapping score.
ω^X and ω^Z are the X and Z components of the relative angular velocity respectively.
EA_X, EA_Y, and EA_Z are the rotation angles around the X, Y, and Z axes respectively.

D. Analysis of Selected Features

We list selected features in the Table VI. Among these features, six features belonged to the proposed 3-D pattern features, which demonstrated that the proposed 3-D pattern features contributed greatly to distinguishing PD patients

TABLE VII
RESULTS ON DIFFERENT DATA SUBSETS

Hand		Features	Total Set (49 PD, 29 HC)	*noSeverePD* (17 PD, 28 HC)
Left	Sensitivity	1-D	$93.8 \pm 5.7\%$	$61.7 \pm 36.1\%$
		Traditional	$89.6 \pm 10.6\%$	$75.0 \pm 29.6\%$
		All	$\mathbf{91.8 \pm 8.4\%}$	$\mathbf{100.0 \pm 0.0\%}$
	Specificity	1-D	$76.0 \pm 14.6\%$	$96.0 \pm 8.9\%$
		Traditional	$80.0 \pm 18.3\%$	$86.7 \pm 13.9\%$
		All	$\mathbf{86.7 \pm 13.9\%}$	$\mathbf{96.7 \pm 7.5\%}$
	Accuracy	1-D	$87.2 \pm 7.7\%$	$82.2 \pm 16.1\%$
		Traditional	$85.9 \pm 10.2\%$	$82.2 \pm 7.0\%$
		All	$\mathbf{89.4 \pm 7.0\%}$	$\mathbf{97.8 \pm 4.5\%}$
	F1 score	1-D	$90.2 \pm 5.5\%$	$69.4 \pm 28.6\%$
		Traditional	$88.8 \pm 7.8\%$	$73.3 \pm 15.7\%$
		All	$\mathbf{91.8 \pm 5.8\%}$	$\mathbf{97.8 \pm 5.0\%}$
Right	Sensitivity	1-D	$93.6 \pm 9.8\%$	$88.3 \pm 16.2\%$
		Traditional	$89.6 \pm 7.9\%$	$58.3 \pm 16.7\%$
		All	$\mathbf{93.8 \pm 5.7\%}$	$\mathbf{95.0 \pm 11.8\%}$
	Specificity	1-D	$90.0 \pm 9.1\%$	$96.7 \pm 7.5\%$
		Traditional	$73.3 \pm 19.0\%$	$\mathbf{100.0 \pm 0.0\%}$
		All	$\mathbf{96.7 \pm 7.5\%}$	$96.7 \pm 7.5\%$
	Accuracy	1-D	$92.3 \pm 3.6\%$	$83.3 \pm 9.1\%$
		Traditional	$93.3 \pm 5.3\%$	$84.4 \pm 6.5\%$
		All	$\mathbf{94.9 \pm 5.3\%}$	$\mathbf{95.6 \pm 8.9\%}$
	F1 score	1-D	$93.6 \pm 3.4\%$	$91.0 \pm 12.5\%$
		Traditional	$87.2 \pm 3.6\%$	$72.5 \pm 14.4\%$
		All	$\mathbf{95.8 \pm 4.3\%}$	$\mathbf{95.0 \pm 11.1\%}$

Numerical values are reported as mean value $\pm$ standard deviation of the five-fold results.
Bold font indicates the highest value.
Traditional features were slowness, hypokinesia, and fatigue features.

from HC. Moreover, we investigated the relationship between the MDS-UPDRS FT score and the selected features. All 3-D pattern features except the normalized first principal component variances of $\boldsymbol{\omega}$ and the number of local minimums of $|\omega|$ less than the lower quartile had low correlations ($|r| < 0.50$) with the MDS-UPDRS FT score, which demonstrated that the proposed 3-D pattern features described FT in a way that is different from traditional features.

E. Benefits of 3-D Pattern Features

We conducted significance testing to investigate whether 3-D pattern features could be used to recognize mild PD patients in our previous work [17] and found that 3-D pattern features performed better than 1-D features at the group level. Moreover, we focus on whether 3-D pattern features were important in classifying PD patients at the individual level in this study. We compared the performance of 1-D features, traditional features, and 3-D features and investigated the effects of 3-D pattern features on the total set and *noSeverePD*.

The results are given in the Table VII. All features performed the best on both the total set and the *noSeverePD* subset among these feature combinations. In addition, the 1-D features performed better than traditional features, except for the left hand on the *noSeverePD* subset, because 1-D features contained the 1-D form of the proposed 3-D pattern feature, e.g. the variational mode decomposition energy entropy of ω^Z. We thus conclude that 3-D pattern features are important in distinguishing PD patients from HC with similar MDS-UPDRS FT scores.

TABLE VIII
COMPARISON WITH RELATED WORKS

Year	Author	Sample Size	Accuracy
2014	Lones [4]	49 PD, 41 HC[a]	$90 - 95\%$
2018	Chao [11]	97 PD, 49 HC[b]	R: 93.5% L: 88.6%
		19 PD, 49 HC[d]	R: 89.7% L: 81.0%
2018	Butt [12]	16 PD, 12 HC[a]	84.17%
2019	Domenico [13]	16 PD, 14 HC[a]	87.1%
2020	Moshkova [14]	16 PD, 16 HC[a]	95.3%
2021	Dai [16]	45 PD, 30 HC[b]	96.0%
	Ours	49 PD, 29 HC[c]	R: 94.9% L: 89.4%
		41 PD, 14 HC[b]	R: 96.4% L: 100.0%
		17 PD, 28 HC[e]	R: 95.0% L: 97.8%

L and R mean left hand and right hand respectively.
[a] refers to a data set that did not mention the score distribution.
[b] refers to a data set that only included PD patients rated above 0 and HC were rated as 0 on the MDS-UPDRS.
[c] refers to a data set that was not filtered.
[d] refers to a data set that included HC rated as 0 and PD rated as 1.
[e] refers to a data set that included HC and PD rated as 0 or 1.

IV. DISCUSSION

A. Comparison With Related Works

In this study, we propose a 3-D FT assessment framework and tested its performance on different data subsets. The present work is compared to related work in Table VIII. Most related work did not mention whether the data were filtered. Other works [11], [16] filtered participants so that all invovled PD patients were rated above 0 and all involved HC were rated as 0 according to the MDS-UPDRS. Moreover, the accuracy of Chao's work [11] was low on the data subset in which PD patients were rated as 1 and HC were rated as 0. To the best of our knowledge, this study was the first to investigate how to distinguish PD patients from HC with similar FT scores. Our work reached a comparable accuracy with related works on the total data set, and reached the highest accuracy on the filtered data set (in which PD patients were rated above 0, HC were rated as 0). The results show that the proposed framework performed well in recognizing mild PD patients by involving 3-D pattern features and could distinguish mild PD patients from HC with similar FT scores.

B. Three-Dimensional Pattern Features

We evaluated FT motion using the proposed 3-D pattern features in a way that is different from traditional features. We found the motor coordination of PD patients was significantly worse than that of HC [17], which might reflect the motor impairment of PD. In addition, the PD patients' relative thumb angular velocity was significantly higher [17]. We considered that the motor function of the forefinger might be impaired more than that of the thumb in mild PD because the impairment of the thumb might be compensated for more easily, owing to the larger cortical control area of the thumb.

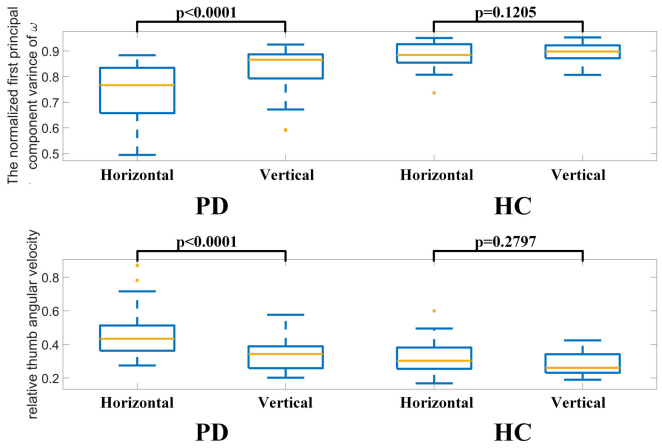

Fig. 3. Comparison of two typical 3-D pattern features in horizontal and vertical tasks for the right hand.

The variational mode decomposition energy entropy of the relative angular velocity components was significantly higher in PD patients than in HC, especially in the case of the Z component ($p < 0.0001$). Higher energy entropy corresponds to more complex FT motions. Overall, the proposed framework performed better with the inclusion of the proposed 3-D pattern features.

C. Effect of Task Type

To the best of our knowledge, no previous research has focused on the effect of the task type. We evaluated our framework on horizontal tasks and vertical tasks and found better performance for the horizontal task. We conducted the paired-sample t-test to investigate the proposed 3-D pattern features in different tasks on the total data set. We found that the horizontal tasks significantly affected PD patients and we presented the results for the right hand in Fig. 3. The results suggested that horizontal tasks might be a better choice when adopting the proposed framework. However, whether the horizontal task is a better choice for FT evaluation in clinical practice needs to be further investigated.

D. Effect of Dominant Hand

All participants in this study were right handed. Similar to [4] and [11], we found that the proposed framework performed better for the right hand on the total data set. But the proposed framework performed better for the left hand on *noSeverePD* subset and filtered subset. Moreover, we investigated the output of the proposed framework for the left and right hands at the individual level and gave the results in the Table IX. The results showed that the proposed framework performed better for the right hand on total data set, but better for the left hand on a subset of the data with less variation between PD patients.

E. Study Limitation

The presented results are promising, yet more research is needed. Validation experiment on larger data set with more mild PD patients is an important part of future work will be used to verify the generalization ability of the proposed framework. Notably, Lones [4] reported that it was easier for classifiers to perform a diagnosis by the dominant hand owing to the association between handedness and the onset side [28]. We obtained similar results, i.e. higher accuracy in right hand for right-handed participants on the total data set, even though the left:right ratio of the onset set in total data set was close to 1:1. It seemed that the association between handedness and the onset side was not the reason for the classifier being more accurate for the dominant hand. This phenomenon needs to be further investigated in clinical practice.

TABLE IX
OUTPUT OF THE PROPOSED FRAMEWORK FOR LEFT AND RIGHT HANDS

Data set	Label	L✓R✓	L✓R✗	L✗R✓	L✗R✗
Total	PD	42	3	4	0
	HC	24	1	4	0
noSeverePD	PD	16	1	0	0
	HC	26	1	1	0
Filtered	PD	41	0	0	0
	HC	12	2	0	0

"L✓R✓" denotes the number of people with correct output for the left and right hands;
"L✓R✗" denotes the number of people with correct output for the left hand and wrong output for the right hands;
"L✗R✓" denotes the number of people with wrong output for the left hand and correct output for the right hands;
"L✗R✗" denotes the number of people with wrong output for the left and right hands.
"*noSeverePD*" refers to a data subset that included HC and PD patients rated as 0 or 1.
"Filtered" refers to a data subset that only included PD patients were rated above 0 and HC were rated as 0.

Lones [4] enrolled only 16 left-handed participants and mixed left-handed and right-handed participants in investigating the performance difference between the dominant hand and non-dominant hands. We considered that the non-dominant hands of right-handed and left-handed people were not comparable, because left-handed people are less lateralized than right-handed people [29]. As in the present study, most previous studies [4], [11], [13], [14], [16] did not investigate the accuracy on left-handed people because of the limited numbers of potential left-handed participants. The performance of the proposed framework on left-handed people needs to be further investigated.

The combination of horizontal tasks and vertical tasks remained a problem because there was a performance gap between horizontal and vertical tasks especially for the right hand. The relationship between horizontal and vertical tasks needs to be further investigated by neurologists in clinical practice.

We did not investigate the effect of the second sensor in this paper because we did not collect the original data of a single sensor during the validation experiment. The effect needs to be further investigated.

V. CONCLUSION

We propose a 3-D FT framework and included 3-D pattern features, namely motor coordination, imbalance impairment, and entropy. We collected and analyzed 3-D FT motion using

the proposed framework. We evaulted the proposed framework on 49 PD patients and 29 HC. The results demonstrated: 1) the proposed 3-D pattern features are not strongly related to traditional features, 2) the proposed framework performed well in recognizing mild PD patients by involving 3-D pattern features, and 3) the proposed framework performed better on horizontal tasks. With the inclusion of 3-D pattern features, the proposed framework could distinguish mild PD patients from HC with aging-related motor decline by single FT motion. The proposed framework can thus be applied to the screening of in PD patients.

ACKNOWLEDGMENT

The authors would like to thank all participants who joined in the validation experiment.

APPENDIX

See Algorithm 1.

REFERENCES

[1] R. B. Postuma et al., "MDS clinical diagnostic criteria for Parkinson's disease," *Movement Disorders*, vol. 30, no. 12, pp. 1591–1601, Oct. 2015.

[2] R. Agostino, A. Berardelli, A. Currá, N. Accornero, and M. Manfredi, "Clinical impairment of sequential finger movements in Parkinson's disease," *Movement Disorders*, vol. 13, no. 3, pp. 418–421, May 1998.

[3] C. G. Goetz et al., "Movement disorder society-sponsored revision of the unified Parkinson's disease rating scale (MDS-UPDRS): Scale presentation and clinimetric testing results," *Movement Disorders*, vol. 23, no. 15, pp. 2129–2170, Nov. 2008.

[4] M. A. Lones et al., "Evolving classifiers to recognize the movement characteristics of Parkinson's disease patients," *IEEE Trans. Evol. Comput.*, vol. 18, no. 4, pp. 559–576, Aug. 2014.

[5] C. H. Adler, J. G. Hentz, J. N. Joyce, T. Beach, and J. N. Caviness, "Motor impairment in normal aging, clinically possible Parkinson's disease, and clinically probable Parkinson's disease: Longitudinal evaluation of a cohort of prospective brain donors," *Parkinsonism Rel. Disorders*, vol. 9, no. 2, pp. 103–110, Dec. 2002.

[6] A. Schrag, "How valid is the clinical diagnosis of Parkinson's disease in the community?" *J. Neurol., Neurosurgery Psychiatry*, vol. 73, no. 5, pp. 529–534, Nov. 2002.

[7] G. Rizzo, M. Copetti, S. Arcuti, D. Martino, A. Fontana, and G. Logroscino, "Accuracy of clinical diagnosis of Parkinson disease," *Neurology*, vol. 86, no. 6, pp. 566–576, Feb. 2016.

[8] O. Rascol, D. J. Brooks, A. D. Korczyn, P. P. De Deyn, C. E. Clarke, and A. E. Lang, "A five-year study of the incidence of dyskinesia in patients with early Parkinson's disease who were treated with ropinirole or levodopa," *New England J. Med.*, vol. 342, no. 20, pp. 1484–1491, May 2000.

[9] Y. Sano et al., "Quantifying Parkinson's disease finger-tapping severity by extracting and synthesizing finger motion properties," *Med. Biol. Eng. Comput.*, vol. 54, no. 6, pp. 953–965, Jun. 2016.

[10] R. Krupicka, S. Viteckova, V. Cejka, O. Klempir, Z. Szabo, and E. Ruzicka, "BradykAn: A motion capture system for objectification of hand motor tests in Parkinson disease," in *Proc. E-Health Bioengineering Conf. (EHB)*, Jun. 2017, pp. 446–449.

[11] C. A. Gao, "Objective assessment of bradykinesia in Parkinson's disease using evolutionary algorithms: Clinical validation," *Translational Neurodegeneration*, vol. 7, no. 1, p. 18, Aug. 2018.

[12] A. H. Butt et al., "Objective and automatic classification of Parkinson disease with leap motion controller," *Biomed. Eng. OnLine*, vol. 17, no. 1, p. 168, Dec. 2018.

[13] D. Buongiorno, I. Bortone, G. D. Cascarano, G. F. Trotta, A. Brunetti, and V. Bevilacqua, "A low-cost vision system based on the analysis of motor features for recognition and severity rating of Parkinson's disease," *BMC Med. Informat. Decis. Making*, vol. 19, no. S9, p. 243, Dec. 2019.

[14] A. Moshkova, A. Samorodov, N. Voinova, A. Volkov, E. Ivanova, and E. Fedotova, "Parkinson's disease detection by using machine learning algorithms and hand movement signal from LeapMotion sensor," in *Proc. 26th Conf. Open Innov. Assoc. (FRUCT)*, Apr. 2020, pp. 321–327.

[15] D. J. Park et al., "Evaluation for parkinsonian bradykinesia by deep learning modeling of kinematic parameters," *J. Neural Transmiss.*, vol. 128, no. 2, pp. 181–189, Feb. 2021.

[16] H. Dai, G. Cai, Z. Lin, Z. Wang, and Q. Ye, "Validation of inertial sensing-based wearable device for tremor and bradykinesia quantification," *IEEE J. Biomed. Health Informat.*, vol. 25, no. 4, pp. 997–1005, Apr. 2021.

[17] J. Li et al., "Three-dimensional pattern features in finger tapping test for patients with Parkinson's disease," in *Proc. 42nd Annu. Int. Conf. IEEE Eng. Med. Biol. Soc. (EMBC)*, Jul. 2020, pp. 3676–3679.

[18] S. A. Ludwig and K. D. Burnham, "Comparison of Euler estimate using extended Kalman filter, madgwick and mahony on quadcopter flight data," in *Proc. Int. Conf. Unmanned Aircr. Syst. (ICUAS)*, Jun. 2018, pp. 1236–1241.

[19] S. Kuchibhotla, H. D. Vankayalapati, and K. R. Anne, "An optimal two stage feature selection for speech emotion recognition using acoustic features," *Int. J. Speech Technol.*, vol. 19, no. 4, pp. 657–667, Dec. 2016.

[20] C. Chang and C. Lin, "LIBSVM," *ACM Trans. Intell. Syst. Technol.*, vol. 2, no. 3, pp. 1–27, 2011.

[21] M. Djurić-Jovičić et al., "Quantification of finger-tapping angle based on wearable sensors," *Sensors*, vol. 17, no. 2, p. 203, Jan. 2017.

[22] M. Yokoe, R. Okuno, T. Hamasaki, Y. Kurachi, K. Akazawa, and S. Sakoda, "Opening velocity, a novel parameter, for finger tapping test in patients with Parkinson's disease," *Parkinsonism Rel. Disorders*, vol. 15, no. 6, pp. 440–444, Jul. 2009.

[23] D. A. Heldman et al., "The modified bradykinesia rating scale for Parkinson's disease: Reliability and comparison with kinematic measures," *Movement Disorders*, vol. 26, no. 10, pp. 1859–1863, Aug. 2011.

[24] Y. Yu, Yudejie, and C. Junsheng, "A roller bearing fault diagnosis method based on EMD energy entropy and ANN," *J. Sound Vibrat.*, vol. 294, nos. 1–2, pp. 269–277, Jun. 2006.

[25] K. Dragomiretskiy and D. Zosso, "Variational mode decomposition," *IEEE Trans. Signal Process.*, vol. 62, no. 3, pp. 531–544, Feb. 2014.

[26] C. A. Hsu, "A practical guide to support vector classication," *Bioinformatics*, vol. 1, pp. 1–16, Apr. 2003.

[27] R. Okuno, M. Yokoe, K. Akazawa, K. Abe, and S. Sakoda, "Finger taps movement acceleration measurement system for quantitative diagnosis of Parkinson's disease," in *Proc. Int. Conf. IEEE Eng. Med. Biol. Soc.*, 2006, pp. 6623–6626.

[28] M. J. Barrett, S. A. Wylie, M. B. Harrison, and G. F. Wooten, "Handedness and motor symptom asymmetry in Parkinson's disease," *J. Neurol., Neurosurgery Psychiatry*, vol. 82, no. 10, pp. 1122–1124, Oct. 2011.

[29] A. J. Marcori and V. H. A. Okazaki, "A historical, systematic review of handedness origins," *Laterality*, vol. 25, no. 1, pp. 87–108, Jan. 2020.